SCIENCE FORUM (JOURNAL OF PURE AND APPLIED SCIENCES) 21 (2021) 503 – 515

http://dx.doi.org/10.5455/sf.87627

Science Forum (Journal of Pure and Applied Sciences)

journal homepage: www.atbuscienceforum.com

On the numerical approximations and simulations of damped and undamped Duffing oscillators

Lydia J. Kwari[1], Joshua Sunday[2*], Joel N. Ndam[2], Adewale A. James[3]

1Department of Mathematics, Federal College of Education, Pankshin, Nigeria

2Department of Mathematics, University of Jos, Jos, Nigeria

3Mathematics Division, American University of Nigeria, Yola, Nigeria

ABSTRACT

The Duffing oscillator (damped or undamped) is one of the most significant and classical nonlinear ordinary differential equations in view of its diverse applications in science and engineering. The Duffing oscillator is an equation that has a cubic stiffness term regardless of the type of damping or excitation. Over the years, different methods have been developed for the solution of Duffing oscillators. In this paper, a new method is derived for the approximation and simulation of damped and undamped Duffing oscillators. In deriving the method, a power series was employed as a basis function by carrying out the integration within one-step interval. The results obtained clearly showed that the method derived is efficient in approximating Duffing oscillators. The phase plots generated equally show that the method is computationally reliable in simulating Duffing oscillators. The paper has further analyzed some properties of the method. The outcome of the analysis shows that the method derived is consistent, convergent, and zero-stable.

ARTICLE INFO

Article history:
Received 12 June 2021
Received in revised form 30 July 2021
Accepted 01 August 2021
Published 12 October 2021
Available online 12 October 2021

KEYWORDS

Approximation
Cubic stiffness
Damping
Duffing oscillator
Oscillation
Simulation

1. Introduction

The major reason why many scientists are inspired by Duffing oscillators is because of their ability to replicate similar dynamics in the natural world. Given their unique characteristics of oscillation and chaotic nature, the Duffing oscillators find applications in the nonlinear vibration of beams and plates (Bakhtiari-Nejad and Nazari, 2009), fluid flow-induced vibration (Srinil and Zanganeh, 2012), large amplitude oscillation of centrifugal governor systems (Younesian et al., 2011) weak signal detection (Abolfazl and Hadi, 2011), and magnetoelastic mechanical systems (Guckenheimer and Holmes, 1983) among others.

In this paper, a method shall be derived for the approximation and simulation of damped and undamped Duffing oscillators of the following form:

$$y''(t)+\rho\, y'(t)+\mu\, y(t)+\gamma\, y^3(t)=F(t) \qquad (1)$$

with the initial following conditions:

$$y(0)=\alpha,\ y'(0)=\beta \qquad (2)$$

where $\alpha,\beta,\rho,\mu,$ *and* γ are real constants and $F(t)$ is a real-valued function. The parameters in Equation (1) are defined explicitly as follows:

- ρ is called the coefficient of damping. It is responsible for controlling the amount of damping.

*** Corresponding author** Joshua Sunday ✉ joshuasunday2000@yahoo.com ✉ Department of Mathematics, University of Jos, Jos, Nigeria; Lydia J. Kwari ✉ lydiakwa01@gmail.com ✉ Department of Mathematics, Federal College of Education, Pankshin, Nigeria.

If $\rho = 0$ then the Duffing oscillator is called undamped, otherwise it is called damped;

- μ is called the linear stiffness coefficient. It controls the linear stiffness of the Duffing oscillator;
- γ is called the nonlinear (harmonic) coefficient which controls the amount of nonlinearity in the restoring force. Note that if $\gamma = 0$, then Duffing oscillator describes a damped and driven simple harmonic oscillator, and
- $F(t)$ is the periodic external driving force of the system which may depend on amplitude and angular frequency.

According to Raisinghania (2014), damping is an influence within or upon the oscillatory system that has the effect of reducing, restricting, or preventing its oscillation. On the other hand, simulation means the use of a mathematical model to recreate a situation, often repeatedly, so that the likelihood of various outcomes can be more accurately estimated. It is also the imitation of the operation of a real-world process or system over time. The behavior of a system that evolves over time is studied by developing a simulation model.

The Duffing oscillator is an example of a dynamical system that exhibits chaotic behavior. For this type of system, there are frequencies at which the vibration suddenly jumps up or down when it is excited harmonically with a slowly changing frequency. The frequencies at which these jumps occur depend upon whether the frequency is increasing or decreasing and whether the nonlinearity is hardening or softening.

It is important to also mention that the physical model depicting the Duffing oscillator involves two magnets that deflect a steel beam toward each other. By applying velocity to the beam, it oscillates between two magnets. The schematic of a Duffing oscillator is shown in Figure 1.

Many researchers have proposed different methods for the solution of Duffing oscillators of the form (1). These methods among others include Laplace decomposition method (Yusufoglu, 2006), restarted Adomian decomposition method (Vahidi et al., 2012), differential transform method (Tabatabaei and Gunerhan, 2014), modified differential transform method (Nourazar and Mirzabeigy, 2013), improved Taylor matrix method (Berna and Mehmet, 2013), variational iteration method (He, 1999, 2000), modified variational iteration method (Goharee and Babolian, 2014), and trigonometrically fitted Obrechkoff method (Shokri et al., 2015) among others. It suffices to say that only few works have been carried out on applying hybrid methods to solve Duffing oscillators. Some of these recent works are those of Sunday (2017) and Khashan et al. (2019).

We assume that the Duffing oscillator in Equation (1) satisfies the existence and uniqueness theorem stated in Theorem 1.

Theorem 1 (Wend, 1967)

Let,

$$u^{(n)} = f(t,u,u',\ldots,u^{(n-1)}),\ u^{(k)}(t_0) = c_k \qquad (3)$$

$k = 0,1,\ldots,(n-1)$, u and f are scalars. Let $\Re$ be the region defined by the inequalities $t_0 \le t \le t_0 + a, |s_j - c_j| \le b,\ j = 0,1,\ldots,(n-1),\ (a>0, b>0)$. Suppose the function $f(t,s_0,s_1,\ldots,s_{n-1})$ is defined in $\Re$ and in addition:

(i) f is non-negative and non-decreasing in each of $f(t,s_0,s_1,\ldots,s_{n-1})$ in $\Re$

(ii) $f(t,c_0,c_1,\ldots,c_{n-1}) > 0$, for $t_0 \le t \le t_0 + a$, and

(iii) $c_k \ge 0,\ k = 0,1,\ldots,n-1$

Then, the Duffing oscillator given by the initial value problem in Equations (1) and (2) has a unique solution in $\Re$. See Wend (1967) for proof.

2. Derivation of the Method and Analysis

We shall derive a new discrete method of the following form:

$$A^{(0)}Y_m^{(i)} = \sum_{i=0}^{1-i} h^i e_i y_n^{(i)} + h^{\mu-i}\left[d_i f(y_n) + b_i f(Y_m)\right] \qquad (4)$$

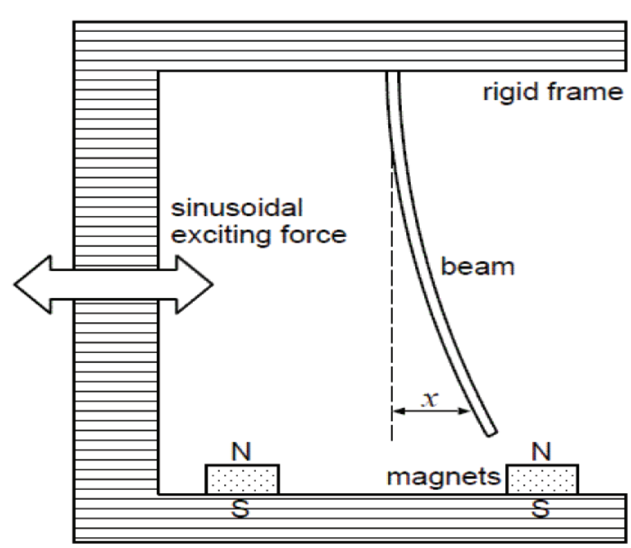

Figure 1. Showing the mechanical interoperation of the Duffing oscillator (Tonya and Anne, 2009).

where

$$Y_m^{(i)} = \left[y_{n+i}^{(i)} \quad y_{n+j}^{(i)} \quad \dots \quad y_{n+1}^{(i)} \right]^T, f(Y_m) = \left[f_{n+i} \quad f_{n+j} \quad \dots \quad f_{n+1} \right]^T,$$

$$y_n^{(i)} = \left[y_{n-i}^{(i)} \quad y_{n-j}^{(i)} \dots y_n^{(i)} \right]^T, f(y_n) = \left[f_{n-i} \quad f_{n-j} \dots \quad f_n \right]^T$$

$A^{(0)} = (r-1)\times(r-1)$ is an identity matrix, μ is the order of the differential equation to be solved, and i in parenthesis, i.e., (i), denotes the power of the derivative of the method. When i = 0, we evaluate the $(r-1)\times(r-1)$ matrices e_0, e_1, d_0 *and* b_0 and when i = 1 (the first derivative), we evaluate the $(r-1)\times(r-1)$ matrices e_1, d_1 *and* b_1.

The major idea in this work is to approximate the exact solution to the Duffing oscillator (1) on the partition, $\pi_{a,b} = [a = x_0 < x_1 < x_2 < \dots < x_n < x_{n+1} < \dots < x_N = b]$ within the one-step integration interval $a,b = [x_n, x_{n+1}]$ by power series polynomial basis function given as follows:

$$y(x) = \sum_{j=0}^{r+s-1} \tau_j x^j \qquad 5)$$

where τ_j is the real coefficients to be determined, s is the number of interpolation points, r is the number of collocation points, and $h = x_n - x_{n-1}$ is a constant step-size of the partition of the interval [a,b]. In doing so, the one-step interval of integration x_n, x_{n+1} shall be partitioned at five off-grid points, i.e., $\frac{1}{6}, \frac{1}{3}, \frac{1}{2}, \frac{2}{3}$, and $\frac{5}{6}$. We assume that the polynomial (5) must pass through the interpolation $(x_{n+s}, y_{n+s}), s = \frac{2}{3}, \frac{5}{6}$ points and the collocation points $(x_{n+r}, f_{n+r}), r = 0 \ \frac{1}{6} \ 1$ which give a system of $(r+s)$ equations as follows:

$$\sum_{j=0}^{r+s-1} \tau_j x^j = y_{n+s},\ s = \frac{2}{3}, \frac{5}{6} \qquad (6)$$

$$\sum_{j=0}^{r+s-1} j(j-1)\tau_j x^{j-2} = f_{n+r},\ r = 0 \ \frac{1}{6} \ 1 \qquad (7)$$

The system of $(r+s)$ Equations in (6) and (7) is then written compactly in the following matrix form:

$$XT = U \qquad (8)$$

where

$$T = [\tau_0 \quad \tau_1 \quad \tau_2 \quad \tau_3 \quad \dots \quad \tau_8]^T, U = \left[y_{n+\frac{2}{3}} \quad y_{\frac{5}{6}} \quad f_n \quad f_{\frac{1}{6}} \quad f_{\frac{1}{3}} \quad f_{\frac{1}{2}} \quad f_{\frac{2}{3}} \quad f_{\frac{5}{6}} \quad f_1 \right]^T$$

and

$$X = \begin{bmatrix} 1 & x_{n+\frac{2}{3}} & x^2_{n+\frac{2}{3}} & x^3_{n+\frac{2}{3}} & x^4_{n+\frac{2}{3}} & x^5_{n+\frac{2}{3}} & x^6_{n+\frac{2}{3}} & x^7_{n+\frac{2}{3}} & x^8_{n+\frac{2}{3}} \\ 1 & x_{n+\frac{5}{6}} & x^2_{n+\frac{5}{6}} & x^3_{n+\frac{5}{6}} & x^4_{n+\frac{5}{6}} & x^5_{n+\frac{5}{6}} & x^6_{n+\frac{5}{6}} & x^7_{n+\frac{5}{6}} & x^8_{n+\frac{5}{6}} \\ 0 & 0 & 2 & 6x_n & 12x_n^2 & 20x_n^3 & 30x_n^4 & 42x_n^5 & 56x_n^6 \\ 0 & 0 & 2 & 6x_{n+\frac{1}{6}} & 12x^2_{n+\frac{1}{6}} & 20x^3_{n+\frac{1}{6}} & 30x^4_{n+\frac{1}{6}} & 42x^5_{n+\frac{1}{6}} & 56x^6_{n+\frac{1}{6}} \\ 0 & 0 & 2 & 6x_{n+\frac{1}{3}} & 12x^2_{n+\frac{1}{3}} & 20x^3_{n+\frac{1}{3}} & 30x^4_{n+\frac{1}{3}} & 42x^5_{n+\frac{1}{3}} & 56x^6_{n+\frac{1}{3}} \\ 0 & 0 & 2 & 6x_{n+\frac{1}{2}} & 12x^2_{n+\frac{1}{2}} & 20x^3_{n+\frac{1}{2}} & 30x^4_{n+\frac{1}{2}} & 42x^5_{n+\frac{1}{2}} & 56x^6_{n+\frac{1}{2}} \\ 0 & 0 & 2 & 6x_{n+\frac{2}{3}} & 12x^2_{n+\frac{2}{3}} & 20x^3_{n+\frac{2}{3}} & 30x^4_{n+\frac{2}{3}} & 42x^5_{n+\frac{2}{3}} & 56x^6_{n+\frac{2}{3}} \\ 0 & 0 & 2 & 6x_{n+\frac{5}{6}} & 12x^2_{n+\frac{5}{6}} & 20x^3_{n+\frac{5}{6}} & 30x^4_{n+\frac{5}{6}} & 42x^5_{n+\frac{5}{6}} & 56x^6_{n+\frac{5}{6}} \\ 0 & 0 & 2 & 6x_{n+1} & 12x_{n+1}^2 & 20x_{n+1}^3 & 30x_{n+1}^4 & 42x_{n+1}^5 & 56x_{n+1}^6 \end{bmatrix}$$

Solving Equation (8) using the Gaussian elimination method for τ_j's which are constants to be determined and substituting into the approximate solution (5) gives a continuous hybrid linear multistep method of the following form:

$$y(x) = \sum_{s=\frac{2}{3},\frac{5}{6}} \alpha_s(x) y_{n+s} + h^2 \left(\sum_{j=0}^{1} \beta_j(x) f_{n+j} + \beta_k(x) f_{n+k} \right), k = \frac{1}{6}, \frac{1}{3}, \frac{1}{2}, \frac{2}{3}, \frac{5}{6} \qquad (9)$$

where

$$\left.\begin{aligned} &\alpha_{\frac{2}{3}}(t) = 5 - 6t \\ &\alpha_{\frac{5}{6}}(t) = 6t - 4 \\ &\beta_0(t) = -\frac{1}{544320}\begin{pmatrix} 629856t^8 + 2939328t^7 - 5715360t^6 + 6001128t^5 \\ -3683232t^4 + 1333584t^3 - 272160t^2 + 129699t \\ -56770 \end{pmatrix} \\ &\beta_{\frac{1}{6}}(t) = -\frac{1}{181440}\begin{pmatrix} 1259712t^8 - 5598720t^7 + 10124352t^6 - 9471168t^5 \\ +4735584t^4 - 1088640t^3 - 160053t + 106190 \end{pmatrix} \\ &\beta_{\frac{1}{3}}(t) = \frac{1}{181440}\begin{pmatrix} 3149280t^8 - 13296960t^7 + 22371552t^6 - 18819864t^5 \\ +7960680t^4 - 1360800t^3 - 524289t + 288470 \end{pmatrix} \\ &\beta_{\frac{1}{2}}(t) = -\frac{1}{272160}\begin{pmatrix} 6298560t^8 - 25194240t^7 + 39517632t^6 - 30373056t^5 \\ +11521440t^4 - 1814400t^3 - 954297t + 534310 \end{pmatrix} \\ &\beta_{\frac{2}{3}}(t) = \frac{1}{181440}\begin{pmatrix} 3149280t^8 - 11897280t^7 + 17472672t^6 - 12532968t^5 \\ +4490640t^4 - 680400t^3 - 530115t + 296450 \end{pmatrix} \\ &\beta_{\frac{5}{6}}(t) = -\frac{1}{181440}\begin{pmatrix} 1259712t^8 - 4478976t^7 + 6205248t^6 - 4245696t^5 \\ +1469664t^4 - 217728t^3 - 198885t + 109550 \end{pmatrix} \\ &\beta_1(t) = \frac{1}{544320}\begin{pmatrix} 629856t^8 - 2099520t^7 + 2776032t^6 - 1837080t^5 \\ +621432t^4 - 90720t^3 - 100737t + 55510 \end{pmatrix} \end{aligned}\right\} \qquad (10)$$

and t s and defined as follows:

$$t = \frac{x - x_n}{h} \qquad (11)$$

Solving independently the solution of (9) for f_{n+j} and f_{n+k} gives the continuous hybrid block method of the following form:

$$Y_{n+j}=\sum_{i=0}^{1}\frac{(jh)^i}{i!}y_n^{(i)}+h^2\left(\sum_{j=0}^{1}\sigma_j(x)f_{n+j}+\sigma_k(x)f_{n+k}\right),\ k=\frac{1}{6},\frac{1}{3},\frac{1}{2},\frac{2}{3},\frac{5}{6} \tag{12}$$

where the coefficients of f_{n+j} and f_{n+k} are given as follows:

$$\left.\begin{aligned}
\sigma_0(t)&=\frac{1}{840}\left(972t^8-4536t^7+8820t^6-9261t^5+5684t^4-2058t^3+420t^2\right)\\
\sigma_{\frac{1}{6}}(t)&=-\frac{3}{70}\left(162t^8-720t^7+1302t^6-1218t^5+609t^4-140t^3\right)\\
\sigma_{\frac{1}{3}}(t)&=\frac{3}{280}\left(1620t^8-6840t^7+11508t^6-9681t^5+4095t^4-700t^3\right)\\
\sigma_{\frac{1}{2}}(t)&=-\frac{1}{105}\left(2430t^8-9720t^7+15246t^6-11718t^5+4445t^4-700t^3\right)\\
\sigma_{\frac{2}{3}}(t)&=\frac{3}{280}\left(1620t^8-6120t^7+8988t^6-6447t^5+2310t^4-350t^3\right)\\
\sigma_{\frac{5}{6}}(t)&=-\frac{3}{70}\left(162t^8-576t^7+798t^6-546t^5+189t^4-28t^3\right)\\
\sigma_1(t)&=\frac{1}{840}\left(972t^8-3240t^7+4284t^6-2835t^5+959t^4-140t^3\right)
\end{aligned}\right\} \tag{13}$$

Evaluating the first derivative of (12) with $t=\frac{1}{6}\left(\frac{1}{6}\right)1$ gives a discrete hybrid block method of the following form (4) where:

$$Y_m^{(i)}=\left[y_{n+\frac{1}{6}}^{(i)}\ y_{n+\frac{1}{3}}^{(i)}\ y_{n+\frac{1}{2}}^{(i)}\ y_{n+\frac{2}{3}}^{(i)}\ y_{n+\frac{5}{6}}^{(i)}\ y_1^{(i)}\right]^T,\ y_n^{(i)}=\left[y_{n-\frac{1}{6}}^{(i)}\ y_{n-\frac{1}{3}}^{(i)}\ y_{n-\frac{1}{2}}^{(i)}\ y_{n-\frac{2}{3}}^{(i)}\ y_{n-\frac{5}{6}}^{(i)}\ y_n^{(i)}\right]^T$$

$$F\left(Y_m\right)=\left[f_{n+\frac{1}{6}}f_{n+\frac{1}{3}}f_{n+\frac{1}{2}}\quad f^2_{n+\frac{2}{3}}f_{n+\frac{5}{6}}f_1\right]^T,\ f\left(y_n\right)=\left[f_{n-\frac{1}{6}}f_{n-\frac{1}{3}}f_{n-\frac{1}{2}}f^T_{n-\frac{2}{3}}f_{n-\frac{5}{6}}f_n\right]^T$$

$A^{(0)}$ is a 6 x 6 identity matrix given as follows:

$$A^{(0)}=\begin{bmatrix}1&0&0&0&0&0\\0&1&0&0&0&0\\0&0&1&0&0&0\\0&0&0&1&0&0\\0&0&0&0&1&0\\0&0&0&0&0&1\end{bmatrix}$$

When $i=0$, we have the following:

$$e_0=\begin{bmatrix}0&0&0&0&0&1\\0&0&0&0&0&1\\0&0&0&0&0&1\\0&0&0&0&0&1\\0&0&0&0&0&1\\0&0&0&0&0&1\end{bmatrix}e_1=\begin{bmatrix}0&0&0&0&0&\frac{1}{6}\\0&0&0&0&0&\frac{1}{3}\\0&0&0&0&0&\frac{1}{2}\\0&0&0&0&0&\frac{2}{3}\\0&0&0&0&0&\frac{5}{6}\\0&0&0&0&0&1\end{bmatrix}d_0=\begin{bmatrix}0&0&0&0&0&\frac{28549}{4354560}\\0&0&0&0&0&\frac{1027}{68040}\\0&0&0&0&0&\frac{253}{10752}\\0&0&0&0&0&\frac{272}{8505}\\0&0&0&0&0&\frac{35225}{870912}\\0&0&0&0&0&\frac{41}{840}\end{bmatrix}$$

$$b_0=\begin{bmatrix}\frac{275}{20736}&-\frac{5717}{483840}&\frac{10621}{1088640}&-\frac{7703}{1451520}&\frac{403}{241920}&-\frac{199}{870912}\\ \frac{97}{1890}&-\frac{2}{81}&\frac{197}{8505}&-\frac{97}{7560}&\frac{23}{5670}&-\frac{19}{34020}\\ \frac{165}{1792}&-\frac{267}{17920}&\frac{5}{128}&-\frac{363}{17920}&\frac{57}{8960}&-\frac{47}{53760}\\ \frac{376}{2835}&-\frac{2}{945}&\frac{656}{8505}&-\frac{2}{81}&\frac{8}{945}&-\frac{2}{1701}\\ \frac{8375}{48384}&\frac{3125}{290304}&\frac{25625}{217728}&\frac{625}{96768}&\frac{275}{20736}&\frac{1375}{870912}\\ \frac{3}{14}&\frac{3}{140}&\frac{17}{105}&\frac{3}{280}&\frac{3}{70}&0\end{bmatrix}$$

When $i=1$, we have the following:

$$e_1=\begin{bmatrix}0&0&0&0&0&1\\0&0&0&0&0&1\\0&0&0&0&0&1\\0&0&0&0&0&1\\0&0&0&0&0&1\\0&0&0&0&0&1\end{bmatrix}d_1=\begin{bmatrix}0&0&0&0&0&\frac{19087}{362880}\\0&0&0&0&0&\frac{1139}{22680}\\0&0&0&0&0&\frac{137}{2688}\\0&0&0&0&0&\frac{143}{2835}\\0&0&0&0&0&\frac{3715}{72576}\\0&0&0&0&0&\frac{41}{840}\end{bmatrix}$$

$$b_1=\begin{bmatrix}\frac{2713}{15120}&-\frac{15487}{120960}&\frac{293}{2835}&-\frac{6737}{120960}&\frac{263}{15120}&-\frac{863}{362880}\\ \frac{47}{189}&\frac{11}{7560}&\frac{166}{2835}&-\frac{269}{7560}&\frac{11}{945}&-\frac{37}{22680}\\ \frac{27}{112}&\frac{387}{4480}&\frac{17}{105}&-\frac{243}{4480}&\frac{9}{560}&-\frac{29}{13440}\\ \frac{232}{945}&\frac{64}{945}&\frac{752}{2835}&\frac{29}{945}&\frac{8}{945}&-\frac{4}{2835}\\ \frac{725}{3024}&\frac{2125}{24192}&\frac{125}{567}&\frac{3875}{24192}&\frac{235}{3024}&-\frac{275}{72576}\\ \frac{9}{35}&\frac{9}{280}&\frac{34}{105}&\frac{9}{280}&\frac{9}{35}&\frac{41}{840}\end{bmatrix}$$

Some properties of the method derived above are analyzed. These properties among others include the order, error constant, consistency, zero-stability, and stability region.

In determining the order and error constant of the method, we first define the linear operator associated with the discrete method (4) as follows:

$$L\{y(t):h\}=A^{(0)}Y_m-\sum_{i=0,\lambda=0}^{1}h^ie_iy_n^{\lambda}+h^2\left[d_0f(y_n)+b_0f(Y_m)\right] \tag{14}$$

Assuming that $y(t)$ is sufficiently differentiable, we write the terms in (14) as a Taylor series expansion about the point t to obtain the following expression:

$$L\left\{y(t):h\right\} = c_0 y(t) + c_1 h y'(t) + c_2 h^2 y''(t) + \ldots$$
$$+ c_p h^p y^p(t) + c_{p+1} h^{p+1} y^{p+1}(t) + c_{p+1} h^{p+2} y^{p+2}(t) \tag{15}$$

where the constant coefficients $c_p, p = 0,1,2,\ldots$ are given as follows:

$$\left.\begin{aligned} c_0 &= \sum_{j=0}^{k} \alpha_j \\ c_1 &= \sum_{j=0}^{k} \left(j\alpha_j - \beta_j \right) \\ &. \\ &. \\ &. \\ c_p &= \sum_{j=0}^{k} \left[\frac{1}{q!} j^q \alpha_j - \frac{1}{(q-1)!} j^{q-1} \beta_j \right], \ q = 2,3,\ldots \end{aligned}\right\} \tag{16}$$

The method (4) is said to be of uniform accurate order ρ, if ρ is the largest positive integer for which $\bar{c}_0 = \bar{c}_1 = \bar{c}_2 = \ldots = \bar{c}_p = \bar{c}_{p+1} = 0, \bar{c}_{p+2} \neq \bar{0} \cdot \bar{c}_{p+2}$. $\bar{c}_{p+2}$ is called the error constant and the local truncation error of the method is given as follows:

$$\bar{t}_{n+k} = \bar{c}_{p+2} h^{(p+2)} y^{(p+2)}(t) + O\left(h^{(p+3)}\right) \tag{17}$$

The order of the method is also defined as the largest positive real number ρ that quantifies the rate of convergence of a numerical approximation of a differential equation to that of the analytical or exact solution.

Definition 1 Error constant (Fatunla, 1980)

The term $\bar{c}_{p+2}$ is called the error constant (Fatunla, 1980). Thus, the local truncation error for (4) is given as follows:

$$t_{n+k} = \bar{c}_{p+2} h^{p+2} y^{(p+2)}(t_n) + o(h^{p+3}) \tag{18}$$

The error constant is the accumulated error when the order of a method has been computed. The order and the error constants of the method derived are summarized in Table 1.

The consistency of the method is now tested. According to Lambert (1991), a continuous linear multistep method is said to be consistent if it satisfies the following condition:

(i) the order $p \geq 1$

Table 1. Order and error constant of the method.

$y(x_{n+j})$	Order	Error constant
$j = \frac{1}{6}$	7	6.5967×10^{-10}
$j = \frac{1}{3}$	7	1.6311×10^{-9}
$j = \frac{1}{2}$	7	2.5516×10^{-9}
$j = \frac{2}{3}$	7	3.4721×10^{-19}
$j = \frac{5}{6}$	7	4.4435×10^{-9}
$j = 1$	7	5.1032×10^{-9}

It is important to state that the consistency of a method controls the magnitude of the local truncation error committed at each stage of the computation. The new method derived is, therefore, consistent since it has a uniform order $p = 7$.

We further test for the zero-stability of the method. According to Fatunla (1980), a method is said to be zero-stable, if the roots $z_s, s = 1,2,\ldots,k$ of the first characteristic polynomial p (z) defined by $\rho(z) = \det(zA^{(0)} - e_0)$ satisfies $|z_s| '' 1$ and every root satisfying $|z_s| = 1$ has multiplicity not exceeding the order of the differential equation. Moreover, as $h \to 0$, $\rho(z) = z^{r-} \ (z-1)$ where μ is the order of the differential equation, r is the order of the matrices $A^{(0)}$ *and* e_0. The main consequence of zero-stability is to control the propagation of the error as the integration progresses.

The first characteristic polynomial of the method derived is as follows:

$$\rho(z) = \left| z \begin{bmatrix} 1&0&0&0&0&0 \\ 0&1&0&0&0&0 \\ 0&0&1&0&0&0 \\ 0&0&0&1&0&0 \\ 0&0&0&0&1&0 \\ 0&0&0&0&0&1 \end{bmatrix} - \begin{bmatrix} 0&0&0&0&0&1 \\ 0&0&0&0&0&1 \\ 0&0&0&0&0&1 \\ 0&0&0&0&0&1 \\ 0&0&0&0&0&1 \\ 0&0&0&0&0&1 \end{bmatrix} \right|$$

$$= \begin{vmatrix} z&0&0&0&0&-1 \\ 0&z&0&0&0&-1 \\ 0&0&z&0&0&-1 \\ 0&0&0&z&0&-1 \\ 0&0&0&0&z&-1 \\ 0&0&0&0&0&z-1 \end{vmatrix} = z^5(z-1)$$

Solving for z in

$$z^5(z-1)=0 \tag{19}$$

we obtain $z_1=0,\ z_2=0,\ z_3=0,\ z_4=0,\ z_5=0$ and $z_6=1$. The method derived is, therefore, zero-stable.

To test for the convergence of the method, we employed Theorem 1.

Theorem 2 (Dahlquist, 1956)

The necessary and sufficient conditions for a linear multistep method to be convergent are that it be consistent and zero-stable.

Thus, the method derived is said to be convergent.

Finally, we determined the region within which the method derived is stable.

Definition 2 Region of Absolute Stability (Yan, 2011)

The region of absolute stability is a region in the complex z plane, where $z=\lambda h$. It is defined as those values of z such that the numerical solutions of $y''=-\lambda^2 y$ satisfy $y_j \to 0$ *as* $j \to \infty$ for any initial condition.

Applying the boundary locus method, we obtained the stability polynomial of the method as follows:

$$\begin{aligned}\bar{h}(w) = {} & h^{12}\left(\frac{1}{426649337856}w^6-\frac{157}{4266493378560}w^5\right)-h^{10}\left(\frac{1943}{63489484800}w^5-\frac{131}{338610585600}w^6\right)\\ & -h^{8}\left(\frac{301}{37791360}w^5-\frac{89}{10581580800}w^6\right)-h^{6}\left(\frac{67}{94058496}w^6+\frac{40613}{47029248}w^5\right)\\ & -h^{4}\left(\frac{6137}{155520}w^5-\frac{41}{311040}w^6\right)-h^{2}\left(\frac{7}{432}w^6+\frac{137}{216}w^5\right)+w^6-2w^5\end{aligned} \tag{20}$$

The stability region of the method is shown in Figure 2.

The region of absolute stability of the method is A-stable. The region of absolute stability is the area within the curve.

3. Numerical Simulation of Duffing Oscillators

In this section, we shall apply the newly derived method in simulating Duffing oscillators. Firstly, the numerical simulation of Duffing oscillators would be carried out to determine the type of spring. Secondly, the Duffing oscillator shall be simulated at varied external force parameter F in order to investigate the influence of F on the behavior of the system.

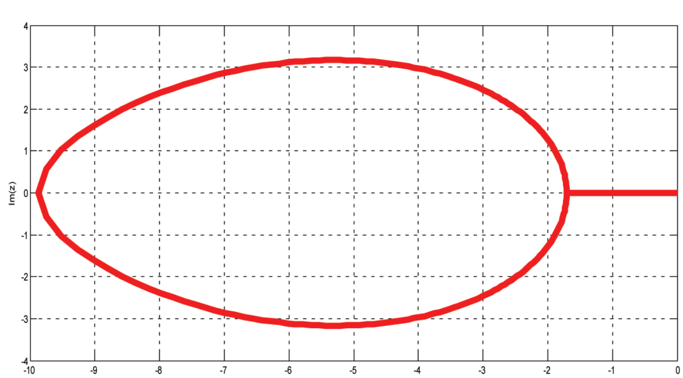

Figure 2. Stability region of the method.

3.1. Numerical simulation of Duffing oscillators to determine the type of springs

According to Zhang (2005), Duffing oscillators could be simulated in order to determine the type of springs. The author, therefore, varied the stiffness coefficient μ and nonlinear coefficient γ. This led to the types of Duffing oscillators presented in Table 2.

Adapted from Zhang (2005).

The new method developed in this research was also used to simulate the Duffing oscillators using the same parameters adopted by Zhang (2005). This is to help in comparing the phase plots of Zhang (2005) with those of the new method. The authors of this study went further to investigate the minimum value of the damping coefficient ρ that is required by each type of Duffing oscillator.

The authors, therefore, modified Table 2 of Zhang (2005) as that shown in Table 3.

A hard spring is stiffer than a soft spring; when a mass is pulled from a hard spring, its shape is restored more quickly than a soft spring and will then oscillate until it reaches its equilibrium. This behavior is evident in Figure 3 as the spring achieves periodic motion quickly (Zhang, 2005). The "tightness" of the path shown in the figure demonstrates the oscillation of the spring, which is relatively close to its equilibrium point.

Figure 5 shows a soft spring. Given its low spring constant value (i.e., low stiffness), it will have difficulty restoring to its initial coiled state.

Table 2. Types of Duffing oscillators.

Type of Duffing oscillator	μ	γ
Hard spring	>0	>0
Soft spring	<0	>0
Non-harmonic spring	>0	=0
Inverted spring	>0	<0

Table 3. Types of Duffing oscillators.

Type of Duffing oscillator	μ	γ	ρ
Hard spring	>0	>0	>0
Soft spring	<0	>0	<0
Non-harmonic spring	>0	=0	>0
Inverted spring	>0	<0	>0

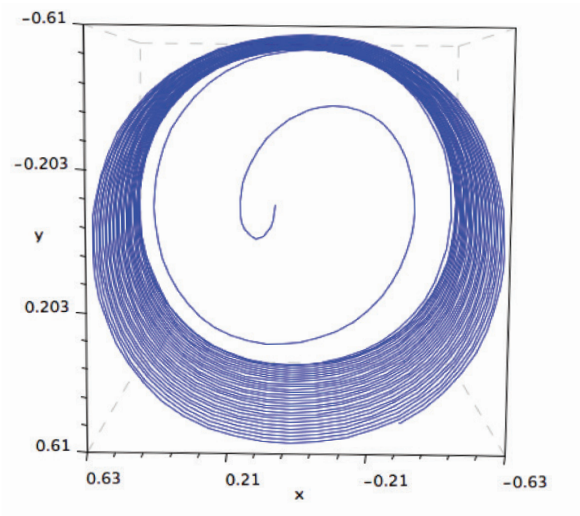

Figure 3. Hard spring with $F = 0.34875,\ \mu = 1(>0),\ \gamma = 1(>0)$ (Zhang, 2005).

A simple harmonic oscillator occurs when the path of the spring moves at a constant frequency and amplitude around its equilibrium point (Zhang, 2005).

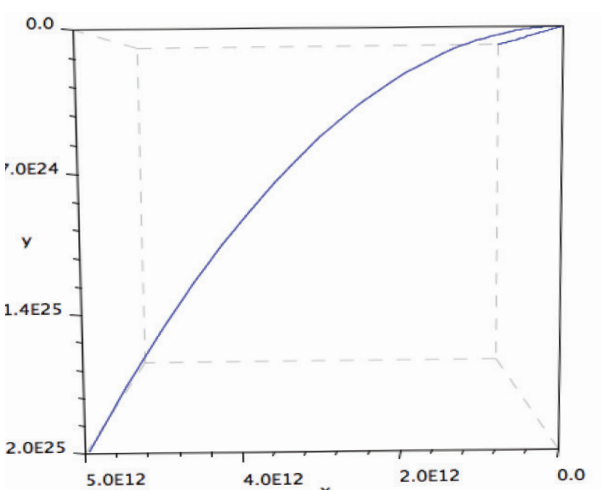

Figure 5. Soft spring with $F = 0.34875, \mu = -1(<0), \gamma = 1(>0)$ (Zhang, 2005).

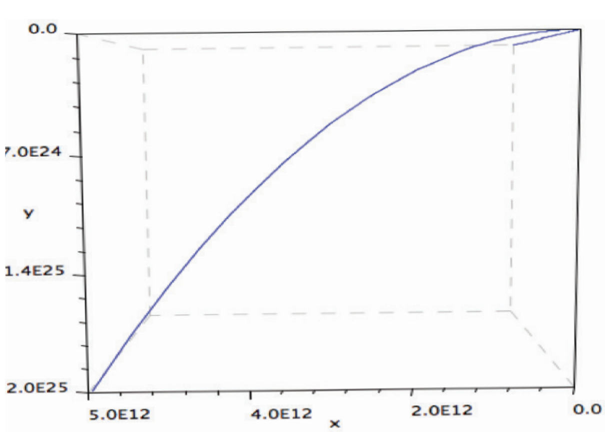

Figure 6. Soft spring with $F = 0.34875, \mu = -1(<0), \gamma = 1(>0), \rho = -0.5(<0)$ using the new method.

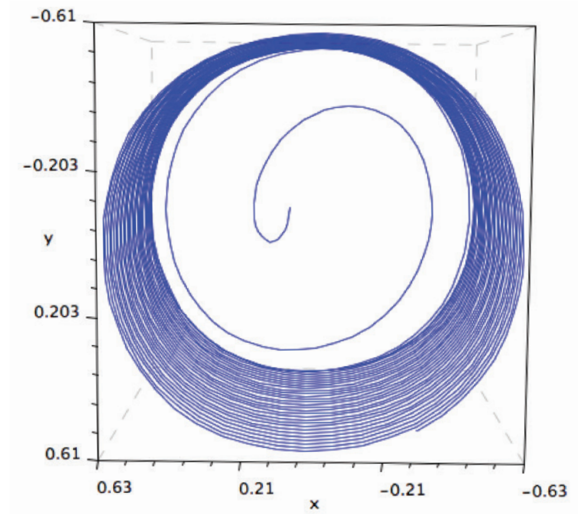

Figure 4. Hard spring with $F = 0.34875, \mu = 1(>0), \gamma = 1(>0), \rho = 0.5(>0)$ using the new method.

If the harmonic oscillator is damped, it is characterized with a decreasing frequency and amplitude over time. Conversely, as shown in Figure 7, this spring is non-harmonic $\gamma = 0$, displaying a lack of balance with respect to the equilibrium point.

Figure 9 shows the system behavior of an inverted spring where its parameters are the opposite of those of a soft spring (Zhang, 2005).

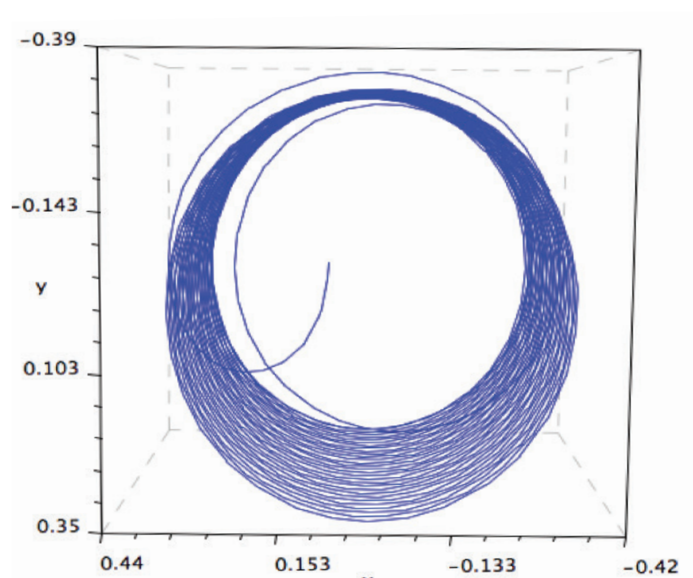

Figure 7. Non-harmonic spring with $F = 0.34875, \mu = 1(>0), \gamma = 0$ (Zhang, 2005).

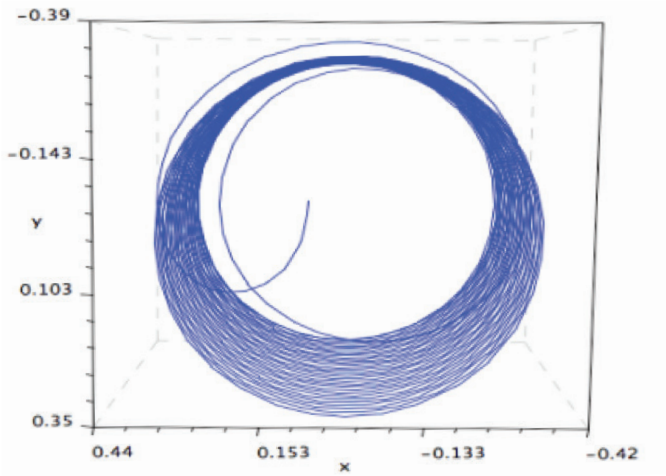

Figure 8. Non-harmonic spring with $F = 0.34875, \mu = 1(>0), \gamma = 0, \rho = 0.5(>0)$ using the new method.

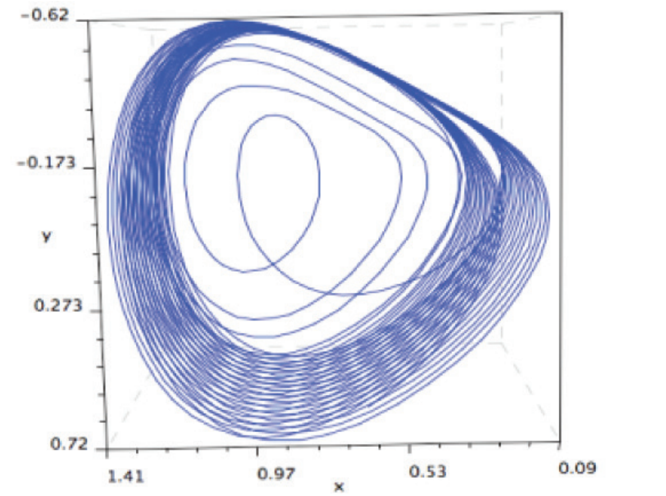

Figure 9. Inverted spring with $F = 0.34875, \mu = 1(>0), \gamma = -1(<0)$ (Zhang, 2005).

3.2. Numerical simulation of Duffing oscillators to investigate the influence of external driving force F

Oscillation is one of the most significant characteristics of the Duffing equation, hence it is alternatively labeled as Duffing oscillator. The property “oscillation” is inherent in the system’s behavior. Therefore, in this section, the method derived shall be used in simulating the Duffing oscillator by varying the external driving force F.

Therefore, the force F would be varied at F = 0.1,10,50,55,60; also, the nonlinear (harmonic) and spring stiffness parameters are set to be equal, i.e., $\quad = \gamma = 1$, while we assume that there is no damping r = 0.

It was, however, observed that a particular F-value offered a distinctive pattern inconsistent with the others. Specifically, *F=55* in Figure 14 shows a highly structured set of trajectories in its phase plot presentation. Unlike other systems with an F-value relatively close to this one (Fig. 13, *F=55* and Fig. 15 *F=60*), this particular system *F=55* appears to have a lesser visible random set of trajectories (Zhang, 2005). With further exploration of random samples of F-values between 70 and 100, no other unique patterns were detected causing a speculation that *F=55* potentially has some algebraic significance.

4. Results and Discussion

The method derived shall be applied in approximating Duffing oscillators of the form (1). The method shall also be used to solve some other types of second-order differential equations. The following notations are used in Tables 4–9.

t = Point of evaluation;

Error = Absolute error of the new method;

EMU = Absolute error in Malik et al. (2015);

EOM = Absolute error in Olabode and Momoh (2016);

ESJ = Absolute error in Sunday (2017);

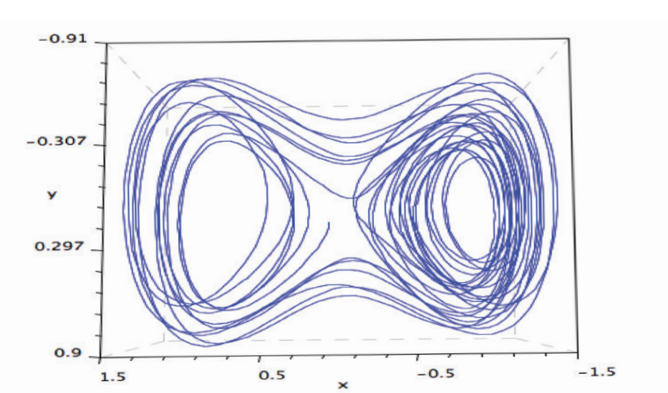

Figure 10. Inverted spring with $F = 0.34875, \mu = 1(>0), \gamma = -1(<0), \rho = 0.5(>0)$ using the new method.

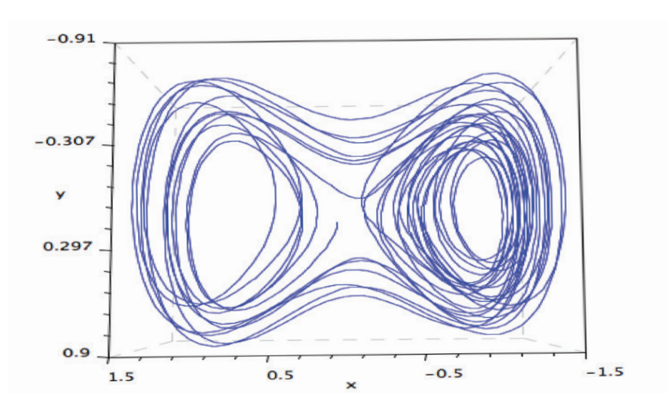

Figure 11. Variance on force $F = 0.1, \mu = 1, \gamma = 1, \rho = 0$ using the new method.

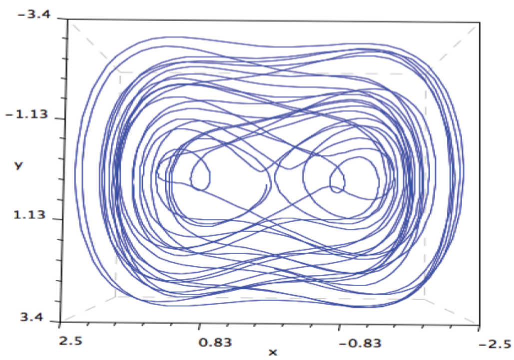

Figure 12. Variance on force $F = 10, \mu = 1, \gamma = 1, \rho = 0$

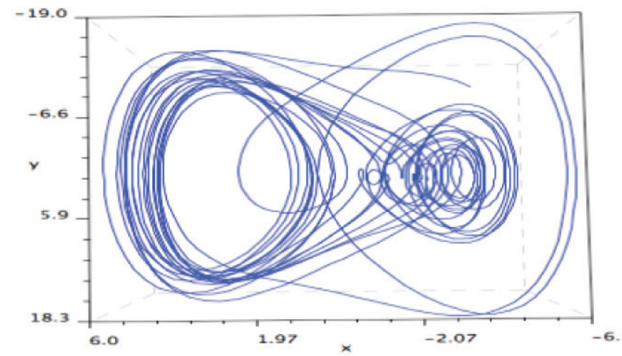

Figure 13. Variance on force $F = 50, \mu = 1, \gamma = 1, \rho = 0$

EOO = Absolute error in Olanegan et al. (2018);

EDR = Absolute error in Dominic (2019);

Time/s = Evaluation time per seconds of the new method.

Problem 1

Consider the damped Duffing oscillator,

$$y''(t) + y'(t) + y(t) + y^3(t) = \cos^3(t) - \sin(t) \quad (21)$$

whose initial conditions are,

$$y(0) = 1, \ y'(0) = 0 \quad (22)$$

The exact solution is given as follows:

$$y(t) = \cos(t) \quad (23)$$

Source: Tabatabaei and Gunerhan (2014)

The result of Problem 1 is presented in Table 4.

Problem 2

Consider the damped Duffing oscillator,

$$y''(t) + 2y'(t) + y(t) + 8y^3(t) = e^{-3t} \quad (24)$$

with the initial conditions,

$$y(0) = \frac{1}{2}, \ y'(0) = -\frac{1}{2} \quad (25)$$

The exact solution is given as follows:

$$y(t) = \frac{1}{2}e^{-t} \quad (26)$$

Source: Malik et al. (2015)

The result of Problem 2 is presented in Table 5.

Problem 3

Consider the following undamped Duffing oscillator of the following form:

$$y''(t) + y(t) + y^3(t) = B\cos\Omega t \quad (27)$$

with initial conditions,

$$y(0) = \alpha, \ y'(0) = 0 \quad (28)$$

where

$$\alpha = 0.200426728067, B = 0.002, \ \Omega = 1.01 \quad (29)$$

The exact solution to the problem is

$$y(t) = \sum_{i=0}^{3} A_{2i+1} Cos\left((2i+1)\Omega t\right) \quad (30)$$

where

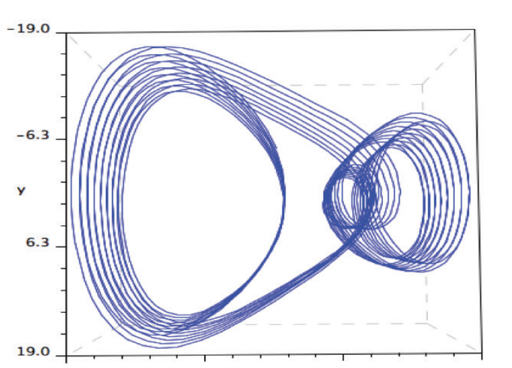

Figure 14. Variance on force $F = 55, \mu = 1, \gamma = 1, \rho = 0$

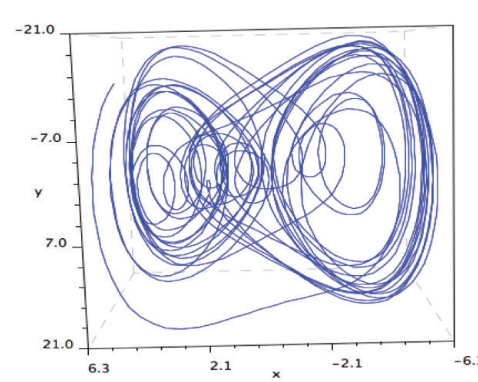

Figure 15. Variance on force $F = 60, \mu = 1, \gamma = 1, \rho = 0$

$$\begin{Bmatrix} A_1, A_3, A_5, \\ A_7, A_9 \end{Bmatrix} = \begin{Bmatrix} 0.200179477536, 0.0024946143, 0.000000304014, \\ 0.000000000374, 0.000000000000 \end{Bmatrix} \quad (31)$$

Source: Shokri et al. (2015)

The result of Problem 3 is presented in Table 6.

Problem 4

Consider the undamped Duffing oscillator,

$$y''(t) + y(t) + y^3(t) = (\cos t + \varepsilon \sin 10t)^3 - 99\varepsilon \sin 10t \quad (32)$$

with the initial conditions,

$$y(0) = 1,\ y'(0) = 10\varepsilon \quad (33)$$

where $\varepsilon = 10^{-10}$. The exact solution is given as follows:

$$y(t) = \cos t + \varepsilon \sin 10t \quad (34)$$

This equation describes a periodic motion of low frequency with a small perturbation of high frequency.

Source: Olabode and Momoh (2016)

The result of Problem 4 is presented in Table 7.

Problem 5

The temperature y degrees of a body, t minutes after being placed in a certain room, satisfiy the differential equation $3\frac{d^2y}{dt^2} + \frac{dy}{dt} = 0$. By using the substitution $z = \frac{dy}{dt}$ or otherwise, find y in terms of t given that $y = 60$ when $t = 0$, $y = 35$, and $t = 6\ln 4$. Find out after how many minutes the rate of cooling of the body will have fallen below one degree per minute, giving your answer correct to the nearest minute. The problem is mathematically modeled as follows:

$$y''(t) = -\frac{y'(t)}{3},\ y(0) = 60, y'(0) = -\frac{80}{9} \quad (35)$$

The exact solution is given by,

$$y(t) = \frac{80}{3} e^{-\left(\frac{1}{3}\right)t} + \frac{100}{3} \quad (36)$$

Source: Olanegan et al. (2018).

The result of Problem 5 is presented in Table 8.

Problem 6

Consider the Stiefel and Bettis system of equations,

$$\begin{aligned} &y''_1(t) + y_1(t) = 0.001\cos(t),\ y_1(0) = 1, y'_1(0) = 0 \\ &y''_2(t) + y_2(t) = 0.001\sin(t),\ y_2(0) = 1, y'_2(0) = 0.9995 \end{aligned} \quad (37)$$

The exact solution is given as follows:

$$\begin{aligned} &y_1(t) = \cos(t) + 0.0005t\sin(t) \\ &y_2(t) = \sin(t) - 0.0005t\cos(t) \end{aligned} \quad (38)$$

Source: Olabode and Momoh (2016)

The result of Problem 6 is presented in Table 9.

Table 4. Showing the results for Problem 1 in comparison with the absolute errors in Sunday (2017).

t	Exact Solution	Computed Solution	Error	ESJ	Time/s
0.1000	0.9950041652780258	0.9950041652780258	0.000000e + 000	9.418022e-013	0.3093
0.2000	0.9800665778412416	0.9800665778412416	0.000000e + 000	9.320766e-012	0.3960
0.3000	0.9553364891256060	0.9553364891256060	0.000000e + 000	2.371603e-011	0.4134
0.4000	0.9210609940028850	0.9210609940028850	0.000000e + 000	4.248379e-011	0.4401
0.5000	0.8775825618903727	0.8775825618903727	0.000000e + 000	6.390422e-011	0.4867
0.6000	0.8253356149096781	0.8253356149096781	0.000000e + 000	8.632239e-011	0.5134
0.7000	0.7648421872844882	0.7648421872844882	0.000000e + 000	1.082653e-010	0.5800
0.8000	0.6967067093471651	0.6967067093471651	0.000000e + 000	1.285219e-010	0.6367
0.9000	0.6216099682706640	0.6216099682706640	0.000000e + 000	1.461836e-010	0.6934
1.0000	0.5403023058681392	0.5403023058681390	0.000000e + 000	1.606468e-010	0.7404

Table 5. Showing the results for Problem 2 in comparison with the absolute errors in Malik et al. (2015).

t	Exact Solution	Computed Solution	Error	ESJ	Time/s
0.1000	0.4524187090179798	0.4524187090179798	0.000000e + 000	1.487e-08	0.1411
0.2000	0.4093653765389909	0.4093653765389909	0.000000e + 000	1.286e-07	0.1904
0.3000	0.3704091103408589	0.3704091103408589	0.000000e + 000	1.464e-07	0.2209
0.4000	0.3351600230178196	0.3351600230178196	0.000000e + 000	1.393e-07	0.2803
0.5000	0.3032653298563167	0.3032653298563167	0.000000e + 000	1.845e-07	0.3269
0.6000	0.2744058180470131	0.2744058180470131	0.000000e + 000	2.422e-07	0.4435
0.7000	0.2482926518957047	0.2482926518957047	0.000000e + 000	2.468e-07	0.4999
0.8000	0.2246644820586107	0.2246644820586107	0.000000e + 000	2.127e-07	0.5866
0.9000	0.2032848298702994	0.2032848298702994	0.000000e + 000	1.987e-07	0.6929
1.0000	0.1839397205857211	0.1839397205857211	0.000000e + 000	2.071e-07	0.7298

Table 6. Showing the results for Problem 3 in comparison with end-point absolute errors in Sunday (2017).

h	Error	ESJ	Time/s
$m/500$	1.256151e-016	8.813783e-013	1.2676
$m/1000$	1.678127e-016	1.114692e-012	1.6272
$m/2000$	2.061690e-015	2.953554e-012	2.1287
$m/3000$	4.167032e-015	2.339406e-012	2.2781
$m/4000$	5.267817e-015	1.859929e-012	3.0182
$m/5000$	6.762717e-015	1.328992e-012	4.0167

m =10 in Table 6.

Table 7. Showing the results for Problem 4 in comparison with the absolute errors in Olabode and Momoh's (2016) study.

t	Exact Solution	Computed Solution	Error	EOM	Time/s
0.0025	0.9999968750041274	0.9999968750041274	0.000000e + 000	0.000000e+000	0.2198
0.0050	0.9999875000310395	0.9999875000310395	0.000000e + 000	1.110223e-016	0.2728
0.0075	0.9999718751393287	0.9999718751393287	0.000000e + 000	8.881784e-016	0.3300
0.0100	0.9999500004266486	0.9999500004266486	0.000000e + 000	7.771561e-016	0.3712
0.0125	0.9999218760297148	0.9999218760297148	0.000000e + 000	4.440892e-016	0.4109
0.0150	0.9998875021243030	0.9998875021243030	0.000000e + 000	9.992007e-016	0.4698
0.0175	0.9998468789252486	0.9998468789252486	0.000000e + 000	1.665335e-015	0.5126
0.0200	0.9998000066864446	0.9998000066864446	0.000000e + 000	2.775558e-015	0.6234
0.0225	0.9997468857008414	0.9997468857008414	0.000000e + 000	5.440093e-015	0.6824
0.0250	0.9996875163004431	0.9996875163004431	0.000000e + 000	7.216450e-015	0.7219
0.0275	0.9996218988563066	0.9996218988563066	0.000000e + 000	9.436896e-015	0.7715

Table 8. Showing the results for Problem 5 in comparison with the absolute errors in Olanegan et al. (2018);

t	Exact Solution	Computed Solution	Error	EOO	Time/s
0.1000	59.1257626795201650	59.1257626795207595	9.245422e-016	7.476427e-06	0.0091
0.2000	58.2801862675098120	58.2801862675098669	7.891086e-016	2.939419e-05	0.0101
0.3000	57.4623311476255910	57.4623311476255318	5.926176e-016	6.480165e-05	0.0200
0.4000	56.6712885078119370	56.6712885078114686	4.684342e-015	1.127905e-05	0.0502
0.5000	55.9061793304163790	55.9061793304166670	3.123519e-015	1.724976e-04	0.1005
0.6000	55.1661534154128500	55.1661534154117978	4.647865e-014	2.431027e-04	0.1267
0.7000	54.4503884356475110	54.4503884356471849	3.261193e-014	3.238270e-04	0.1956
0.8000	53.7580890230573020	53.7580890230571750	2.845575e-014	4.139307e-04	0.2601
0.9000	53.0884858848458170	53.0884858848457003	1.167002e-014	5.127120e-04	0.3001
1.0000	52.4408349486343820	52.4408349486341820	3.638386e-013	6.195049e-04	0.3721

Table 9. Showing the results for Problem 6 in comparison with the absolute errors in Dominic's (2019).

t	Error *y*1	Error *y*2	Error in EDR *y*1	Error in EDR *y*2	Time/s
0.1000	1.256535e-012	2.826929e-012	1.055952e-012	1.016920e-011	0.0321
0.2000	2.113954e-012	5.899430e-012	1.428503e-011	2.038960e-011	0.0493
0.3000	2.376410e-012	6.830921e-012	4.955660e-011	1.545070e-013	0.0667
0.4000	3.424150e-012	1.499123e-012	1.016060e-010	8.106310e-011	0.1056
0.5000	3.394396e-012	1.839452e-012	1.741578e-010	2.537670e-010	0.1229
0.6000	3.343548e-012	1.655884e-011	2.642489e-010	5.484820e-010	0.1419
0.7000	4.294920e-012	1.247034e-011	3.757940e-010	9.957060e-010	0.1594
0.8000	4.257394e-012	8.431255e-011	5.060214e-010	1.625950e-009	0.1766
0.9000	5.234413e-012	5.323966e-011	6.590353e-010	2.469720e-009	0.1939
1.0000	6.226530e-012	3.212587e-011	8.322541e-010	3.557520e-009	0.2985

From the results obtained in Tables 4–9, it is obvious that the method derived performed better than the ones with which we compared our results. The simulations results obtained from the phase plots in Figures 3–15 equally showed that the newly derived method effectively simulates Duffing oscillators. This is because by varying parameters, we can know the resultant type of Duffing oscillator. It also tells us the effect of external driving force F on the behavior of the system. The method derived was also employed in solving other types of second-order differential equations and from the results obtained; it is obvious that the method is computationally reliable. The evaluation time per seconds of the new method was also micro, implying that the method generates results very fast. Thus, it can be concluded that the method is efficient.

5. Conclusion

Conclusively, a method has been derived for the approximation and simulation of Duffing oscillators of the form (1). It is clear that the method is computationally reliable by virtue of the results obtained. Furthermore, some basic properties of the method were analyzed and from the analysis carried out, the method was found to be convergent, consistent and zero-stable.

References

Abolfazl J, Hadi F. The application of Duffing oscillator in weak signal detection. ECTI Trans Electr Eng Electron Commun 2011; 9(1):1–6.

Bakhtiari-Nejad F, Nazari M. Nonlinear vibration analysis of isotropic cantilever plate with visco-elastic laminate. Nonlinear Dyn 2009; 56:325–56.

Berna B, Mehmet S. Numerical solution of Duffing equations by using an improved Taylor matrix method. J Appl Math 2013; 2013:1–6; doi:10.1155/2013/691614

Dahlquist GG. Convergence and stability in the numerical integration of ordinary differential equations. Math Scand 1956; 4:33–50.

Dominic R. A class of implicit third derivative hybrid method for the solution of initial value problems of ordinary differential equations. PhD Thesis, Adamawa State University Mubi, Mubi, Nigeria, 2019.

Fatunla SO. Numerical integrators for stiff and highly oscillatory differential equations. Math Comput, 1980; 34:373–90.

Goharee F, Babolian E. Modified variational iteration method for solving Duffing equations. Indian J Sci Res 2014; 6(1):25–9.

Guckenheimer J, Holmes P. Nonlinear oscillations, dynamical systems and bifurcations of vector fields. Springer-Verlag, Berlin, Germany, 1983.

He JH. Variational iteration method for autonomous ordinary differential systems. Appl Math Comput 2000; 114:115–23.

He JH. Variational iteration method. A kind of nonlinear analytical technique. Int J Non Mech 1999; 34:699–708.

Khashan MM, Syam MI, Alomari AK. Numerical solution of cubic free undamped Duffing oscillator equation using continuous implicit hybrid method. Ital J Pure Appl Math 2019; 42:588–97.

Lambert JD. Numerical methods for ordinary differential systems: the initial value problem. John Wiley and Sons LTD, Chichester, UK, 1991.

Malik SA, Ullah A, Qureshi IM, Amir M. Numerical solution of Duffing equation using hybrid genetic algorithm technique. MAGNT Res Rep, 2015; 3(2):21–30.

Nourazar S, Mirzabeigy A. Approximate solution for nonlinear Duffing oscillator with damping effect using the modified differential transform method. Sci Iran B 2013; 20(2):364–8.

Olabode BT, Momoh AL. Continuous hybrid multistep methods with Legendre basis function for direct treatment of second order stiff ordinary differential equations. Am J Comput Appl Math 2016; 6(2):38–49; doi:10.5923/j.ajcam.20160602.03

Olanegan OO, Ogunware BG, Alakofa CO. Implicit hybrid points approach for solving general second order ordinary differential equations with initial values. J Adv Math Comput Sci 2018; 27(3):1–14; doi:10.9734/JAMCS/2018/40447

Raisinghania MD. Ordinary and partial differential equations. Revised edition, S. Chand and Company LTD, New-Delhi, India, 2014.

Shokri A, Shokri AA, Mostafavi S, Sa'adat H. Trigonometrically fitted two-step Obrechkoff methods for the numerical solution of periodic initial value problems. Iran J Math Chem 2015; 6(2):145–61.

Srinil N, Zanganeh H. Modeling of coupled cross-flow/in-line vortex-induced vibrations using double Duffing and Vander pol oscillators. Ocean Eng 2012; 53:83–97.

Sunday J. The Duffing oscillator: applications and computational simulations. Asian Res J Math 2017; 2(3):1–13; doi:10.9734/ARJOM/2017/31199

Tabatabaei K, Gunerhan E. Numerical solution of Duffing equation by the differential transform method. Appl Math Inf Sci Lett 2014; 2(1):1–6; doi:10.12785amisl/020101

Tonya D, Anne MM. The Duffing equation: a nonlinear differential equation. Term project on ordinary differential equations. Georgia Gwinneth College, Mississippi, USA, 2009.

Vahidi AR, Azimzadeh Z, Mohammadifar S. Restarted adomian decomposition method for solving Duffing-van der pol equation. Appl Math Sci 2012; 6(11):499–507.

Wend DVV. Uniqueness of solution of ordinary differential equations. Am Math Mon 1967; 74(8):27–33.

Yan YL. Numerical methods for differential equations. City University of Hong-Kong, Kowloon, Hong-Kong, 2011.

Younesian D, Askari H, Saadatnia Z, Yazdi MK. Periodic solutions for nonlinear oscillation of a centrifugal governor system using the He's frequency-amplitude formulation and He's energy balance method. Nonlinear Science Letters A 2011; 2:143–8.

Yusufoglu E. Numerical solution of Duffing equation by the Laplace decomposition algorithm. Appl Math Comput 2006; 177(2):572–80.

Zhang WB. Differential equations, bifurcations, and chaos in economics. World Scientific Publishing, Hackensack, NJ, 2005.